Chain Architecture Effects on Deformation and Fracture of Block Copolymers with Unentangled Matrices

Chang Y. Ryu,[§] Janne Ruokolainen, Glenn H. Fredrickson, and Edward J. Kramer*

Departments of Materials and Chemical Engineering, University of California, Santa Barbara, California 93106

Stephen F. Hahn

Corporate R&D, The Dow Chemical Company, Midland, Michigan 48674

Received September 5, 2001

ABSTRACT: We investigate the influence of chain architecture on the microscopic deformation and fracture mechanisms of poly(vinylcyclohexane)−poly(ethylene) (PCHE−PE) block copolymer thin films. To investigate the correlation between the mechanical and fracture properties of the polymer and its chain architecture, a "metal grid technique" was employed to apply tensile tension on the thin films of PCHE homopolymer ($\bar{M}_w$ = 283 000 g/mol), ordered PCHE−PE−PCHE triblock (CEC; $\bar{M}_w$ = 107 000 g/mol and f_{PE} = 0.29 by weight), and PCHE−PE−PCHE−PE−PCHE pentablock (CECEC; $\bar{M}_w$ = 110 000 g/mol and f_{PE} = 0.30 by weight) copolymers. We observe that both PCHE and CEC deform plastically by crazing. The median strain for crazing of the CEC is 1.3%, whereas that for PCHE is 0.7%. The extension ratio of the crazes λ_{craze} also decreases from 8.4 (PCHE) to 4.3 (CEC), indicating that the PE midblock dramatically decreases λ_{craze}. Both PCHE and CEC crazes, however, eventually break down to form cracks at relatively small strains. The mechanism of deformation and fracture changes dramatically for the pentablock copolymer, CECEC. This pentablock deforms primarily by the formation of shear deformation zones at a median strain of about 2.1%, but crazing competes with shear deformation and crazes with tips blunted by shear deformation zones are frequently observed. We do not observe any significant craze or deformation zone breakdown in the CECEC even at strains up to 23%. Therefore, while maintaining the total M_w and f_{PE} nearly unchanged, a "brittle-to-ductile" transition is caused by changing the chain architecture from triblock to pentablock. Because the PCHE midblock chains in CECEC can form bridging chains between highly entangled PE domains, we attribute the ductility of CECEC primarily to the increase in the network density that disfavors both craze formation and premature craze breakdown.

Introduction

Many glassy amorphous polymers with otherwise desirable characteristics are very brittle even at rather large molecular weights. Often this brittleness can be traced to a low entangled strand density (high entanglement molecular weight M_e), which predisposes the glassy polymer to form weak crazes that break down readily to form cracks. Polymers with a high entangled strand density (low entanglement molecular weight M_e) tend to form shear deformation zones (DZs) rather than crazes.[1] In this regard cross-linked network strands and entangled network strands behave identically so that cross-linking can convert a polymer that crazes in tension, and whose crazes break down to form cracks, into a polymer that deforms only by forming DZs that are immune to breakdown.[2] In the glassy state the network (entanglements and cross-links) not only controls the deformation mechanism but also determines its extensibility. Glassy polymers with a lower entanglement density (high M_e) have higher extension ratios and lower volume fractions of craze fibrils.[3]

Block copolymers have the potential for altering dramatically the simple picture sketched above for glassy homopolymers. The block domain size is of the same order as the typical craze fibril spacing; the flow and cavitation stress of different domains can be quite disparate, and the entanglement network within different domains can be very dissimilar. A proper molecular design of block copolymers is essential in developing new block copolymer materials with desirable properties, because block copolymers can have a wide range of properties depending on molecular weight, composition, and chain architecture.[4,5] Morphology certainly plays an important role in controlling the final mechanical properties of a block copolymer. For example, Weidisch et al.[6,7] showed that mechanical properties, such as Young's modulus and tensile strength, of poly(styrene-*b*-*n*-butyl methacrylate) PS−P*n*BMA diblock copolymers do not change monotonically with block copolymer composition. Although P*n*BMA is less tough than PS, they found out that a PS−P*n*BMA diblock copolymer containing 26 vol % P*n*BMA is even tougher than PS homopolymer. For a given morphology and composition, chain architecture of the block copolymer also strongly affects its mechanical properties. For example, a poly(styrene-*b*-isoprene) PS−PI diblock copolymer with a composition of 17 wt % PS behaves similar to a viscoelastic fluid, whereas its matched PS−PI−PS triblock copolymer with the same composition and morphology as the PS−PI diblock becomes an elastomeric network ($G' \sim \omega^0$) at room temperature.[8] This elasticity of the triblock copolymer derives from the fact that the rubbery PI midblock chain is not permitted to relax due to attached glassy PS blocks at both its ends.

Semicrystalline−amorphous block copolymers can be subdivided into two different classes depending on

§ Current address: Department of Chemistry, Rensselaer Polytechnic Institute, Troy, NY 12180.

* Corresponding author.

10.1021/ma011576r CCC: $22.00
Published on Web 02/13/2002

Table 1. Molecular Weights and Compositions of PCHE Homopolymers and PCHE−PE Block Copolymers

polymer	chain architecture	$\bar{M}_w$, g/mol	f_{PE}, wt %	$\bar{M}_w/\bar{M}_n$	M_w of PCHE block, g/mol	M_w of PE block, g/mol	crystallinity of PE (wt %) by DSC[d]	crystallinity of PE (wt %) by WAXS[e]
PCHE	homopolymer	283 000	0	2.2[a]	283 000			
CEC	triblock[b]	107 000	29	1.04	38 000	31 000	25	19
CECEC	pentablock[c]	110 000	30	1.18	26 000	17 000	23	13

[a] $\bar{M}_n$(PCHE) = 129 000 g/mol. [b] PCHE−PE−PCHE triblock copolymer. [c] PCHE−PE−PCHE−PE−PCHE pentablock copolymer. [d] Differential scanning calorimetry. [e] Wide-angle X-ray scattering.

whether crystallization is coupled with or decoupled from microphase separation. When the glass transition temperature T_g of an amorphous block is higher than the melting temperature of the semicrystalline block T_m (i.e., $T_g > T_m$), a confined crystallization of the semicrystalline block occurs within the ordered domains formed by microphase separation.[9] Because the amorphous block is glassy (i.e., vitrified) at the crystallization temperature, junction points between blocks are immobilized, and the microstructures of the block copolymers are unaffected by the quenching kinetics. However, the crystallinity of the semicrystalline blocks is usually smaller that the crystallinity resulting from unconfined crystallization of the homopolymer. The crystallinity in the confined block may also be affected by thermal history. On the contrary, when the T_g of the amorphous block is lower than the T_m of the semicrystalline block ($T_g < T_m$), the crystallization of the semicrystalline block occurs when the amorphous block is rubbery (i.e., mobile). The domain structure of such a semicrystalline−rubbery block copolymer is often disturbed by growth of semicrystalline lamellae. The extent of such disturbance depends on quenching kinetics.[10]

Poly(vinylcyclohexane) or poly(cyclohexylethylene) (PCHE) is a glassy amorphous polymer that has desirable optical and thermal properties. It has excellent clarity, excellent UV stability, low birefringence, and a high glass transition temperature T_g of about 145 °C.[11−13] However, its large M_e (49 000 g/mol)[12,14] means that PCHE is also extremely brittle. One method of relieving this undesirable brittleness of PCHE, while retaining a relatively high modulus and optical clarity, is to form block copolymers whose microstructure consists of poly(ethylene) (PE) domains in a PCHE matrix. The semicrystalline PE block can be synthesized by hydrogenation of 1,4-polybutadiene (PB), with a minimum (about 10%) 1,2-polybutadiene content. Block copolymers of PCHE and PE can be produced by hydrogenation of PS and PB block copolymer precursors synthesized by anionic polymerization. This synthesis scheme is an economically attractable route due to the low cost of the monomers. Because M_e of PE (hydrogenated PB) is about 1200 g/mol,[14] the PE block is highly entangled and ductile. These PCHE−PE block copolymer materials are optically clear and can exhibit practical toughness at relatively low molecular weights, making them easy to process.

In this paper, we report on the microscopic deformation and fracture mechanisms of glassy PCHE and how these are affected by inserting one or two short semicrystalline blocks of PE that form cylindrical domains in the PCHE matrix. These mechanisms of PCHE, PCHE−PE−PCHE (CEC) triblock, and PCHE−PE−PCHE−PE−PCHE (CECEC) pentablock copolymers are investigated by optical and transmission electron microscopy. We demonstrate that, by controlling the molecular architecture of the PCHE−PE block copolymers, these mechanisms can be manipulated to achieve substantial ductility.

Experiments

Materials. The molecular weights and compositions of the PCHE homopolymer and PCHE−PE block copolymers used in this study are listed in Table 1. They were synthesized by heterogeneous catalytic hydrogenation[15] of polystyrene (PS) homopolymer and PS−polybutadiene (PB) block copolymer precursors. The PE blocks contain an average of 26 ethyl branches per 1000 backbone carbons that arise from the 10% 1,2 monomer addition in the PB block.

Tensile Deformation Using the Copper Grid Technique. The deformation and fracture mechanisms of the polymers were investigated using the copper grid technique,[1] whereby many square patches of thin polymer film are simultaneously plastically deformed independently under tension. The copper grid technique utilizes the uniform plastic deformation of an annealed copper grid frame to provide controlled deformation of polymer films that have been bonded to the grid.

Uniform thin films of the block copolymers (thickness = 0.5−0.7 μm) were spun-cast from hot decahydronaphthalene (mixture of *cis*- and *trans*-decalin, Aldrich) solutions on hot sodium chloride crystal substrates at 2500 rpm. The temperature of the substrates was controlled to be about 120 °C by utilizing an IR lamp with a voltage regulator. Uniform thin films of PCHE homopolymers were spun-cast from toluene solutions at room temperature. The block copolymer thin films were then annealed at 190 °C for 3 days under high vacuum ($<10^{-7}$ Torr) and slowly cooled to room temperature at about −0.5 °C/min. These annealing and cooling conditions were chosen to induce embrittlement of the copolymers due to domain reorganization, physical aging, and slow crystallization if such embrittlement is possible. The effect of less severe thermal histories on the deformation and fracture of CEC (there is no significant effect on the CECEC) will be discussed in a future paper.[25] The annealed thin films were then floated off sodium chloride onto the surface of a water bath. These films were then picked up on ductile copper grids, which have been previously annealed at 600 °C for 10 min under vacuum to recrystallize the copper. The grid bars had been coated with PCHE homopolymer prior to the pickup. Bonding of the films to the grid was achieved by a short exposure (~10 s) to toluene vapor. The film squares bonded to the grid were subsequently dried under vacuum ($<10^{-3}$ Torr) for 2 days to remove residual toluene, and the grid was then deformed at room temperature in tension at a slow strain rate of about 4×10^{-4} s^{-1} to various strains. Individual film squares in the copper grid were inspected periodically with a reflection optical microscope to determine for each grid square the strain at the onset of crazing or shear deformation, and the strain at which at the first breakdown of a craze or DZ to form a crack was observed.[6] A typical square was carefully cut from the grid by severing the surrounding grid bars with a razor blade so it could be examined by transmission electron microscopy. One of the advantages of the copper grid technique is that the deformed structures in each grid could be examined by TEM without removing the stress on the sample, because the plastically deformed copper grid maintains the stress developed in the polymer films.

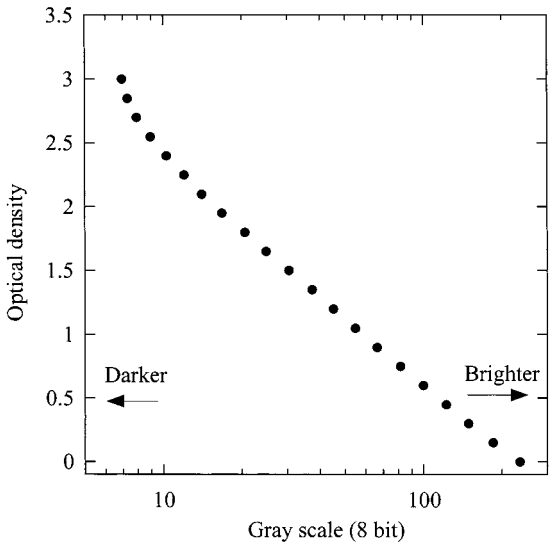

Figure 1. Optical density calibration from the standard negative image as a function of gray scales of scanned image (8 bit).

Scanning Force Microscopy and Transmission Electron Microscopy. The domain structures of the microphase-separated block copolymers were characterized by tapping mode scanning force microscopy (SFM) using a Digital Instrument Dimension 3000. Because of the mechanical contrast between glassy PCHE and the softer PE domains at room temperature, SFM was able to image the microphase-separated domains at the surfaces of annealed thin films of the CEC and CECEC block copolymers. The structure of the highly deformed regions in polymer films from the copper grid experiment was investigated by transmission electron microscopy (TEM) using a JEOL 2000FX TEM operating at 200 kV. Since the polymer films are bonded to the plastically deformed copper grid squares, TEM investigation allows us to examine the deformed structures of the polymer thin films under tension.

Electron Microscopy Image Analysis. Brown[16] and Lauterwasser and Kramer[17] independently developed a method for measuring the extension ratio of crazes, λ_{craze}, from the optical densities of the craze, the film, and a hole in the film using microdensitometry of the electron image plates. Instead of using a microdensitometer, we have employed a digital scanner to estimate the optical densities (which are linearly proportional to the mass−thickness contrast of polymer film) from the gray scales in scanned TEM images. An Epson Expression 1600 scanner was used to scan TEM negative films (as a positive transparency) in order to digitize these images into an 8-bit gray scale. A calibration curve relating these gray scale values to optical density was constructed by scanning a transmission projection step wedge (21 steps, increment of optical density of 0.15) from Stouffer Graphic Arts Equipment Co. Then the optical densities of different regions in the scanned TEM images were estimated from the calibration

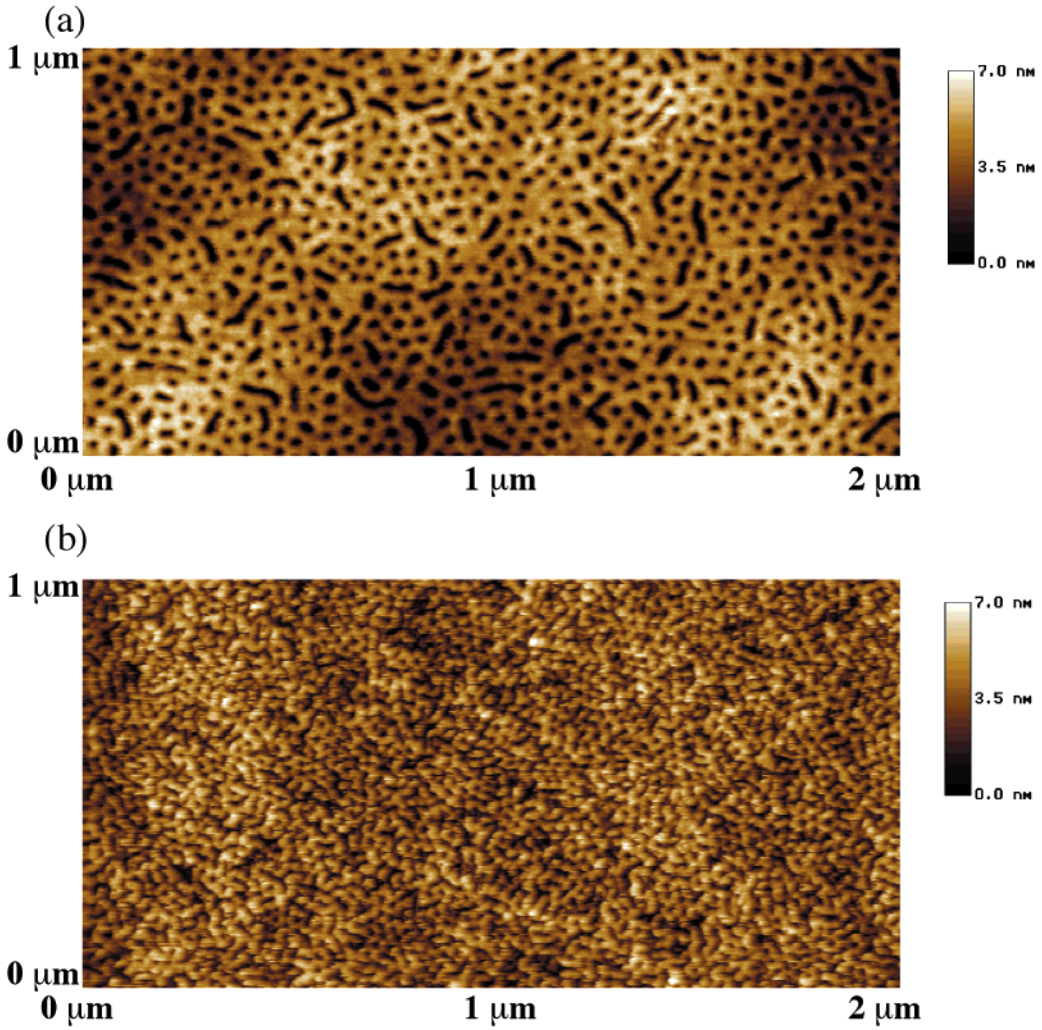

Figure 2. Typical tapping mode AFM images in height scale for (a) CEC and (b) CECEC. PCHE domains appear brighter (higher height), and PE domains appear darker, because the AFM tip can penetrate further into the softer PE domains.

curve and used to estimate the extension ratios of the deformed regions of the sample. In theory, for a good scanner, the optical density vs gray scale should be linear in log scale. Figure 1 is our scanner calibration curve, and it is quite linear up to optical density of 2. Therefore, the TEM image exposure time was carefully controlled, so that we can analyze the optical densities of various features (holes, film, crazes, and/or DZs) only for those negatives where exposure of all these regions were within a linear response region of the negative.

Results and Discussion

Crystallinity and Domain Structures of the CEC and CECEC Block Copolymers. As shown in Table 1, the crystallinity of the PE domains in the CEC and CECEC block copolymers is rather low: 25 wt % by differential scanning calorimetry (DSC) and 19 wt % by wide-angle X-ray scattering (WAXS) in the PE domains of the CEC; 23 wt % by DSC and 13 wt % by WAXS in those of the CECEC. The smaller crystallinities as measured by WAXS than DSC is probably due to the very small crystallite size imposed by the domain size and the surrounding rigid PCHE matrix during crystallization. These crystallinities are about half those that would be obtained from homopolymer PE with the same ethyl branch content. Very similar results are reported by Weimann et al.[9] Since the PE domains are predominately amorphous, with a T_g well below room temperature, they are quite soft mechanically and are easy to image using tapping mode scanning force microscopy (SFM). Figure 2 shows typical tapping mode SFM images of the spin-cast films of CEC and CECEC after annealing on the sodium chloride crystal. The PE domains appear dark in the height image of the tapping mode SFM because the SFM tip at the moderately hard tapping used penetrates more deeply into the softer PE than into the harder surrounding glassy PCHE.[18,19] In both CEC and CECEC the PE domains are cylinders oriented predominately normal to the film surface. Our identification of these domains as the cylinders expected given the 30 wt % PE content of both block copolymers is verified by TEM observations of films stained with RuO_4. While it is unusual to find block copolymers where cylinders in films align normal to the film surface, we believe in this case that the surface energies of the PCHE and the PE are very closely matched. As shown by Russell and co-workers[20,21] in such cases, the block copolymer domains prefer to orient normal to the surface and substrates rather than create islands and holes. When the 1,2-PB content of the precursor is increased from 10 to 40 wt %, keeping the f_{PE} the same, we observe that the cylinders now lie parallel to the surface and attribute this change to a decrease in the PE domain surface energy caused by the additional surface-active methyl groups of more numerous ethyl branches. As seen in Figure 2, neither domain structure is completely uniform, either in orientation or in domain size. This poor organization probably reflects the very high order−disorder transition temperature (>300 °C) for these very high molecular weight copolymers. The self-diffusion for such systems tends to be very slow, and the structures present after spin-casting can become kinetically trapped. If anything, the CECEC shows less well-organized cylinders than the CEC, perhaps because of its more complex architecture.

The scale of the domain structure is rather smaller for the CECEC with respect to the CEC. This difference in scale is expected since the total molecular weights of the two block copolymers are nearly identical. As shown in Table 1, the molecular weight of the PE block in the CEC is 31 000 while that of the PE domains in the CECEC is 17 000. The scale of the PE domains in the CEC should be larger than that of the PE domains in the CECEC given this difference in M_w of the blocks.

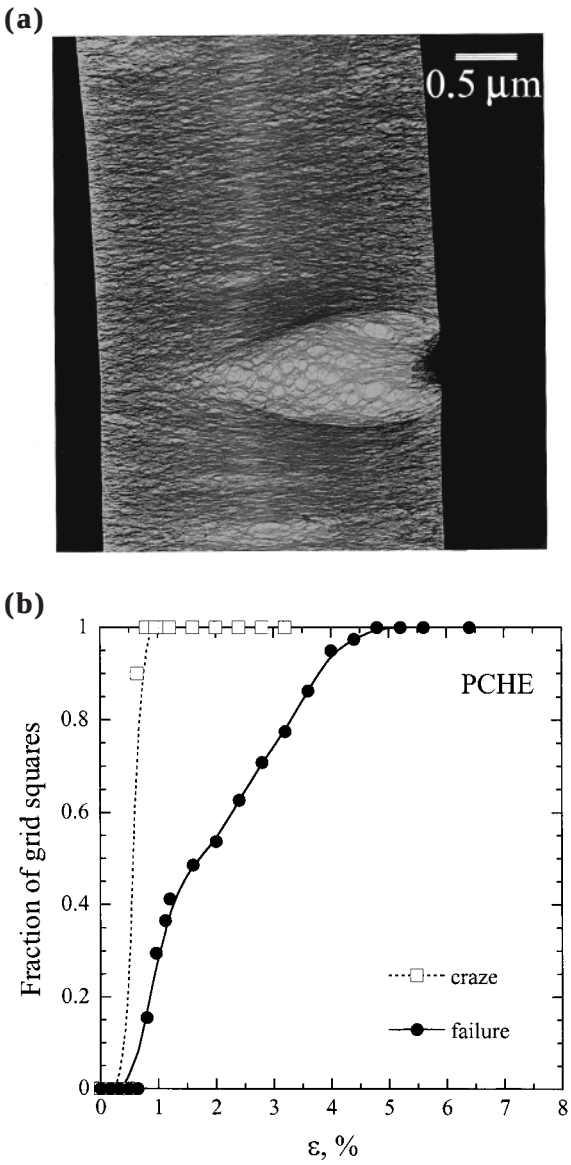

Figure 3. (a) Transmission electron micrograph showing the craze microstructure in a PCHE film at a strain of 3%. (b) Cumulative number fraction of PCHE film squares that have crazed and failed as a function of strain.

Homopolymer PCHE Plastic Deformation and Fracture. PCHE undergoes plastic deformation by crazing with a median onset strain for crazing of about 0.7%. The craze morphology (fibril and void structure) in PCHE is qualitatively similar to that of many other glassy polymers, and the PCHE craze fibrils break down to form cracks in much the same way as do crazes in these other glassy polymers. A pear-shaped void starts at the craze interface and grows slowly as a subcritical crack as the film square is strained further (Figure 3a). This TEM image reveals the typical features of the craze, which consists of small fibrils (ca. 10 nm diameter) that are interconnected by crosstie fibrils embedded in a continuous void space.

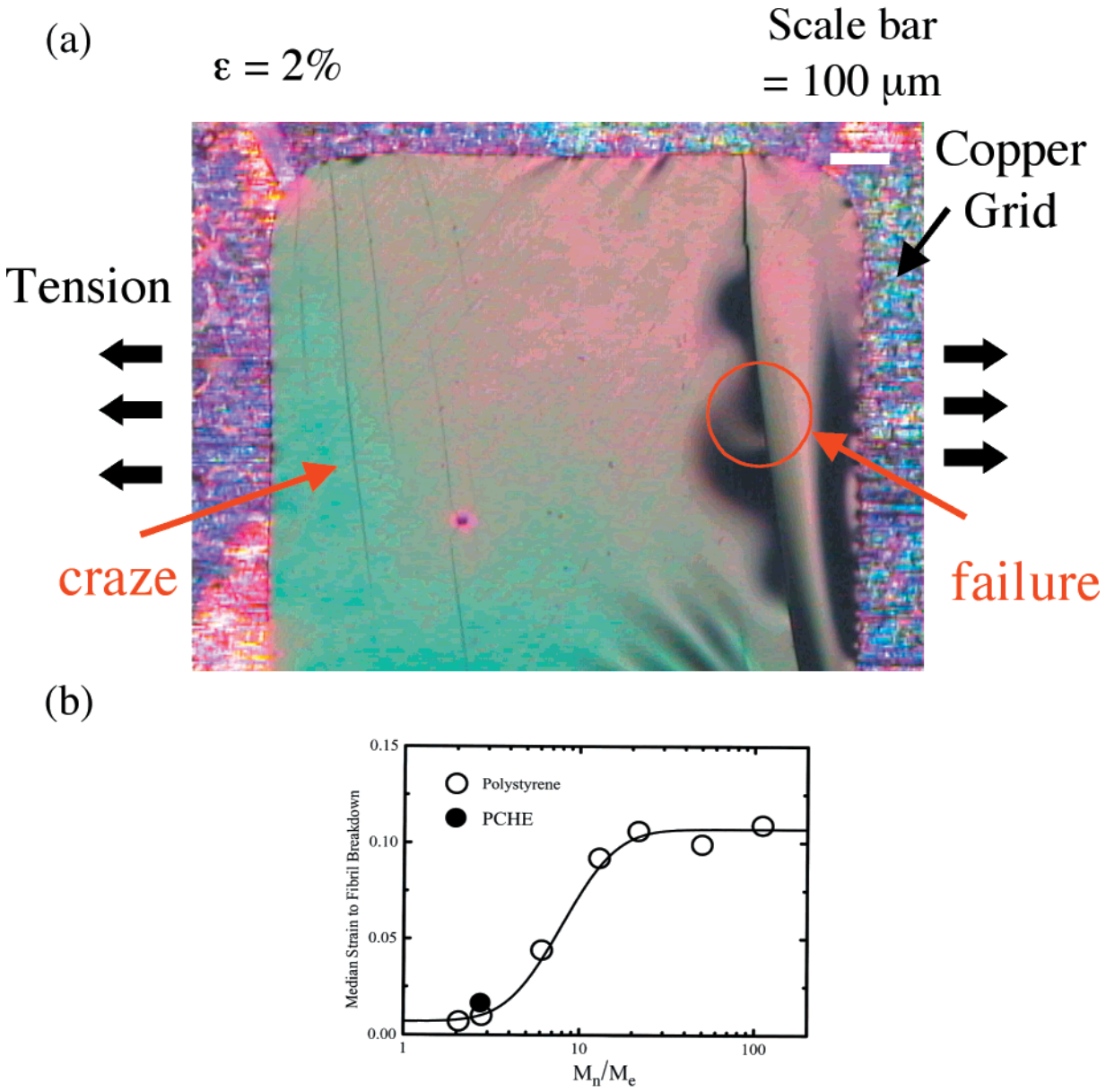

Figure 4. (a) Reflective optical micrograph of a PCHE film under tension at a strain of 2%. (b) Median strain to fibril breakdown of polystyrene as a function of the ratio M_n/M_e (from ref 24). Open points represent PS and the solid point is PCHE.

More quantitative data on deformation and fracture of PCHE are obtained by observing multi-film-square samples using reflection optical microscopy. Reflection optical microscopy allows us to examine the polymer films under tension in-situ. At regular strain intervals, the number fractions of grid squares displaying crazing and fracture (breakdown of craze fibrils) of PCHE are measured, and the results of these measurements are shown in Figure 3b. The median craze breakdown strain ϵ_b for this high molecular weight PCHE is only about 1.8%. Because crazes consist of tiny interconnected fibrils and voids, they scatter light strongly. Therefore, as shown in Figure 4a, they can be easily identified in the reflection optical microscopy experiments by dark lines in the clear film of PCHE. The detection of craze breakdown is also possible with the reflection optical microscope, because the nearby film deforms out of the plane and thus is nonreflecting.

An important determinant of craze fibril stability is the craze fibril volume fraction v_f or its inverse λ_{craze}, which is the craze extension ratio (Table 2). In TEM the electron beam current density imaged after passing through the objective aperture is exponentially attenuated according to the thickness and density of of the polymer located along its path (mass−thickness contrast). If the exposure time of the TEM image is adjusted to fall within the linear response regime of the sensitivity curve of the electron image plate, the optical density produced in the emulsion on the image plate is linearly proportional to the electron beam current density. After obtaining the optical densities of the craze (ϕ_{cr}), the film (ϕ_f), and a hole in the film (ϕ_h) from the electron image plate locally, the relationship

Table 2. Values of Various Parameters of PCHE Homopolymers and PCHE−PE Block Copolymers

polymer	l_e (nm)	λ_{max}	λ_{craze}	λ_{DZ}
PCHE	110	8.5	8.4	
CEC			4.3	
CECEC			3.9	3.1

$$v_f = \frac{1}{\lambda_{craze}} = 1 - \frac{\ln(\phi_{cr}/\phi_f)}{\ln(\phi_h/\phi_f)} \quad (1)$$

then gives v_f or λ_{craze}.[1,17]

A maximum theoretical extension ratio of a single polymer strand in the polymer entanglement network, λ_{max}, is calculated by assuming no slippage between chains (i.e., treating entanglements as permanent cross-links). Using this assumption,

$$\lambda_{max} = l_e/d \quad (2)$$

where d represents the root-mean-square end-to-end distance of a strand of the entanglement molecular weight M_e. Because M_e = 49 000 g/mol and $d = 0.568\sqrt{M_e(\text{g/mol})}$ (Å), the value of d is 130 Å for PCHE.[14] The extended chain contour length between entanglements is

$$l_e = l_0 \frac{M_e}{M_0} \quad (3)$$

where l_0 and M_0 are the average projected length of a stiff extended unit along the chain and its molecular weight, respectively. When we choose M_0 = 110 g/mol, which is the molecular weight of PCHE repeating unit, l_0 is about 2.5 Å and l_e is 1100 Å for PCHE. We found that the theoretical λ_{max} of PCHE is 8.5 and is in good agreement of the experimental λ_{craze}, which is 8.4, from the optical density analysis of TEM negatives. This kind of good agreement between λ_{max} and λ_{craze} has been observed for a wide range of glassy polymers and copolymers[22] and polymer blends.[23] For example, λ_{max} and λ_{craze} of polystyrene (M_e = 17 000 g/mol)[14] are 4.2 and 4.0, respectively.[3] Because $l_e \sim M_e$ and $d \sim M_e^{1/2}$, glassy polymers with high M_e, such as PCHE, have a high value of λ_{max}. The higher the extension ratio λ is, the lower the volume fraction of fibrils in the craze $v_f \sim 1/\lambda$ and the higher the true stress in the polymer fibrils.[3] There is however an additional reason for the very low value of the median strain ϵ_b for fibril breakdown exhibited by PCHE. Previous experiments on polystyrene PS and other glassy polymers[1] have demonstrated that ϵ_b depends on the ratio of the number-average molecular weight M_n of the polymer to M_e. As shown in Figure 4b,[24] the low median strain for fibril breakdown for the PCHE (M_n = 129 000, M_n/M_e = 2.6) is very similar to that of PS with the same value of M_n/M_e. Thus, the brittleness of PCHE does not seem at all unusual.

Triblock Copolymer CEC Plastic Deformation and Fracture. The PCHE−PE−PCHE triblock copolymer (CEC, M = 107 000 g/mol and f_{PE} = 0.29 by weight) deforms plastically by crazing (Figure 5a) in a manner superficially similar to the PCHE homopolymer. However, optical microscopy study reveals that a delicate difference exists in deformation and fracture behavior between the PCHE homopolymer and the CEC triblock copolymer. Figure 6 displays a series of reflection optical microscopy images of CEC deformed in tension to various strains. The distinctive features in the deformation of the CEC triblock copolymer compared to the PCHE homopolymer are wide crazes and localized fibril breakdown as highlighted in Figure 6b,c. The median strain for crazing (~1.6%) for CEC is higher than that for PCHE. While some of the increase may be accounted for by a decrease in modulus, the insertion of the short PE block into the PCHE increases the resistance of the CEC to crazing. Nevertheless, the median strain for craze breakdown of CEC is only 3.3%, about double its value in PCHE but still disappointingly low. The triblock copolymer CEC is nearly as susceptible to craze breakdown as PCHE, and the incorporation of a single PE block in the center of a PCHE chain is not enough to improve significantly the fracture properties of the PCHE-based system.

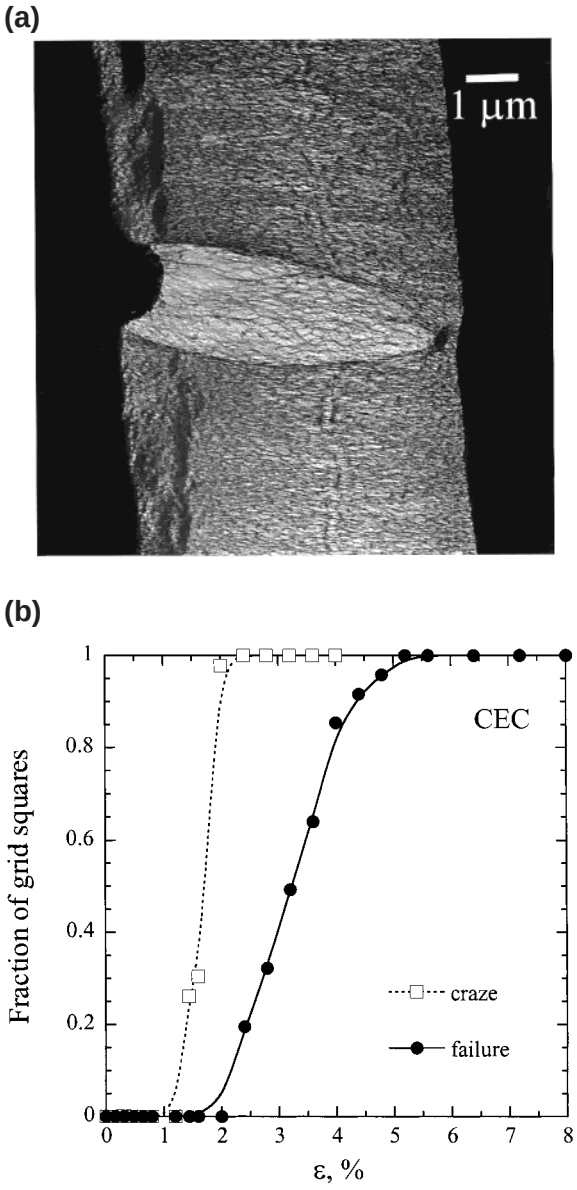

Figure 5. (a) Transmission electron micrograph showing the craze microstructure in a CEC film at a strain of 10%. (b) Cumulative number fraction of CEC film squares that have crazed and failed as a function of strain.

It is significant to note that under other thermal histories (elimination of either the prolonged annealing at 190 °C or the slow cooling from this annealing temperature) the CEC can show a strong resistance to craze breakdown and considerable ductility. The reasons for the extreme sensitivity of the CEC to the annealing treatment and to quenching rate will be discussed in future papers.[25,26] For now it suffices to compare this behavior of CEC with the quite different behavior of the CECEC given the same embrittling thermal treatment.

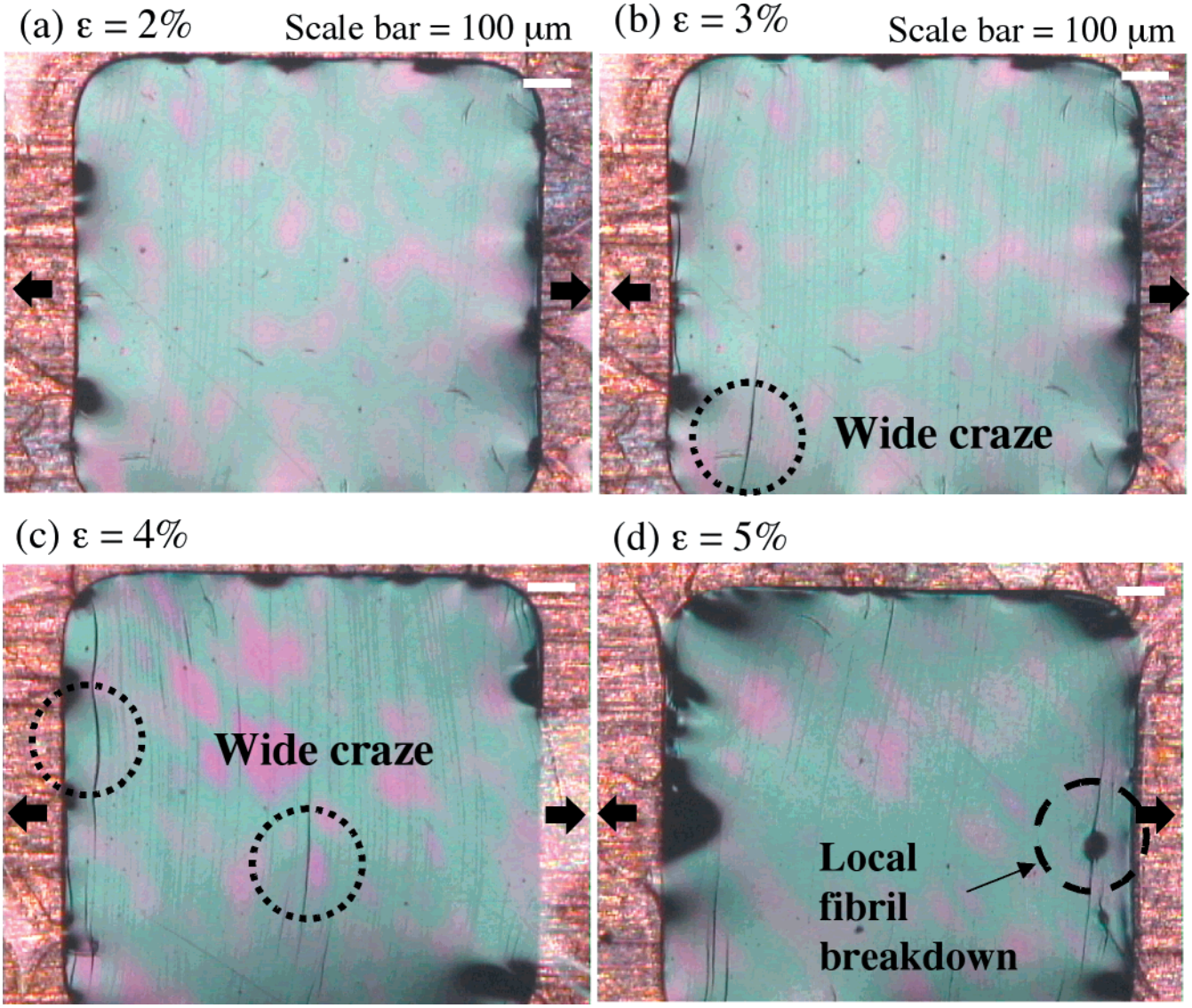

Figure 6. Reflective optical micrographs for the same CEC film under strain at different strains of (a) 2%, (b) 3%, (c) 4%, and (d) 5%.

Pentablock Copolymer CECEC Plastic Deformation and Fracture. The major mechanism of deformation and fracture changes dramatically for the PCHE−PE−PCHE−PE−PCHE pentablock copolymer (CECEC, $M = 110\,000$ g/mol and $f_{PE} = 0.30$ by weight). Note that its total molecular weight and PE content are very similar to those of CEC. As shown in Figure 7, CECEC deforms primarily by the formation of shear deformation zones (DZs) with a median onset strain of about 2.5%. We also frequently observed coexisting shear deformation zones and crazes and crazes whose tips were blunted by shear deformation zones (Figure 8). The overall competition between deformation zones and crazing is similar to that observed [5] for glassy polymers with a network (entangled and/or cross-linked) strand density of about 8×10^{25} strands/m^3. Our most remarkable finding though is that CECEC does not show any significant craze or deformation zone breakdown up to strains of 23% where the copper grid undergoes ductile failure by necking.

The CECEC pentablock copolymer behaves in a ductile manner in the test, despite the fact that its PCHE blocks are shorter than either the brittle PCHE homopolymer or the PCHE blocks of the craze breakdown prone CEC triblock copolymer. The PCHE blocks of the CECEC have a molecular weight well below the entanglement molecular weight of PCHE (49 000 g/mol). The remarkable toughness of CECEC cannot be attributed to the easy deformation of the PE domains, since the volume fraction of PE is nearly identical between CEC and CECEC. Because the domain structure of both block copolymers consists of the same kind of cylindrical PE domains in a glassy PCHE matrix, a difference in the domain structure is also unlikely to be responsible for the toughness.

We propose that the bridging PCHE midblock chains in the CECEC pentablock copolymer produce an increase in the effective entanglement density of the copolymer. These midblock chains bridge between highly entangled PE cylinders and thus prevent easy propagation of fracture though the PCHE matrix domain. These bridging chains are necessarily absent in the CEC triblock copolymer. For the purposes of estimation we can find an effective entanglement density by averaging over both the PE and PCHE domains. The entanglement strand density of PCHE homopolymer (uncorrected for chain ends), ν_e, is 1.1×10^{25} chains/m^3 from its density of 0.92 g/cm^3, so the fact that crazing is the

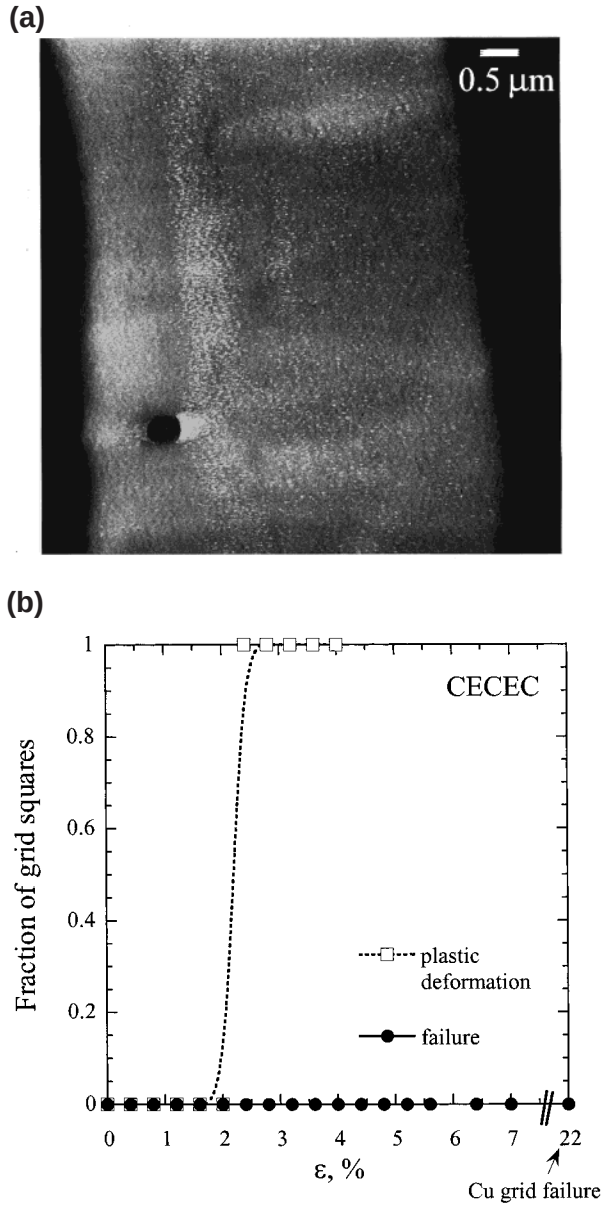

Figure 7. (a) Transmission electron micrograph showing shear deformation zones in a CECEC film at a strain of 6.4%. (b) Cumulative number fraction of CECEC film squares that have undergone plastic deformation (either crazes or DZs) and failure as a function of strain.

dominant deformation mechanism of the homopolymer is not surprising.

If both entanglements in PE and bridging chains in PCHE can serve as cross-links, the effective network strand density ν_e^{eff} for CECEC can be estimated by the additive relationship

$$\nu_e^{eff} = \nu_e^{PE} + \nu_{bridge}^{PCHE} \tag{4}$$

By assuming no chain end effects, the entanglement strand density in the PE domains ν_e^{PE} is calculated by

$$\nu_e^{PE} = f_{PE}\frac{\rho^{PE}N_A}{M_e^{PE}} \tag{5}$$

where f_{PE} and N_A represent weight fraction of PE in CECEC and Avogadro's number, respectively. By estimating the density ρ^{PE} and entanglement molecular weight M_e^{PE} of PE (26 ethyl branches per 1000 backbone carbons) to be 0.785 g/cm^3 and 1200 g/mol,[14] we obtain $\nu_e^{PE} = 11.8 \times 10^{25}$ chains/m^3.

Figure 8. Transmission electron micrograph of CECEC craze with a tip blunted by a shear deformation zone.

The bridging strand density of PCHE midblock chains ν_{bridge}^{PCHE} is estimated by

$$\nu_{bridge}^{PCHE} = f_{PCHE}\frac{\rho^{PCHE}N_A}{M^{PCHE}}\psi_{bridge} \tag{6}$$

where f_{PCHE} and M^{PCHE} represent the weight fraction and the total molecular weight of PCHE in a single chain of CECEC, respectively. Because there is only one PCHE midblock per one chain of CECEC, M^{PCHE} is conveniently used to calculate the strand density of PCHE midblock. Because only a certain fraction ψ_{bridge} of the PCHE midblock chains form bridging chains between PE domains, we must estimate ψ_{bridge} to calculate ν_{bridge}^{PCHE}. Using estimates based on self-consistent-field calculations for the PCHE domains,[27] we choose $\psi_{bridge} = 0.6$, which yields $\nu_{bridge}^{PCHE} = 0.3 \times 10^{25}$ chains/m^3. The total strand density ν_e^{eff} is 12×10^{25} chains/m^3, a value that for a homopolymer would strongly disfavor crazing with respect to formation of shear deformation zones.[2] The resistance to the CECEC to crazing is thus not too surprising.

However, we find that ν_{bridge}^{PCHE} is only 3% of ν_e^{eff} raising the question of why such a tiny increase in strand density should cause such a large change in plastic deformation and fracture behavior from CEC to CECEC. Even though the total network strand density is affected negligibly by the bridged midblock, these bridging chains enable the transfer of stress from one PE domain to its neighbor and prevent the failure of the block copolymer by crack propagation entirely within the PCHE matrix. In support of this idea, we can estimate the force per unit area, $\sigma_{theoretical}$, to break the bridging chains in the PCHE domain (Figure 9). The number of

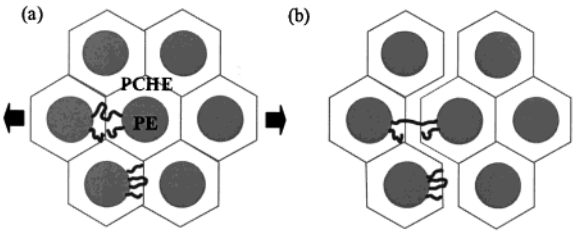

Figure 9. Schematics showing the role of bridging PCHE chains in CECEC.

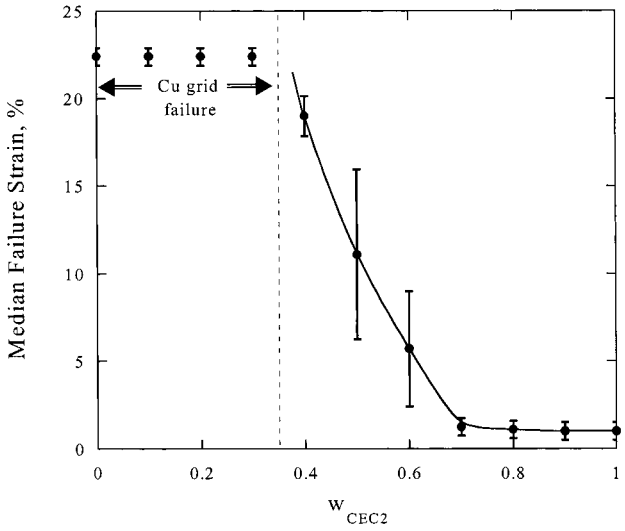

Figure 10. Median strain for craze breakdown for blends of CECEC and CEC2 as a function of the CEC2 weight fraction in the blend of CECEC and CEC2. The error bar represents the standard deviation of measured median failure strains for each blend composition.

bridging chains per unit area in the PCHE matrix Σ is estimated to be 0.04 chains/nm^2, while the force to break a single chain f_b is about 2 nN[28] such that $\sigma_{theoretical} = f_b\Sigma = 80$ MPa, which is well above the yield stress of the PE (~25 MPa).[29] Although CEC has nearly the same ν_E as CECEC, the absence of the bridging midblock chains for CEC means that voiding and cracking within the PCHE domain of the CEC can occur relatively easily.

We did one final set of experiments to test the idea that the midblock chains of the CECEC are crucial to its ductility. We made blends of CECEC with a CEC (CEC2) of lower molecular weight than the CEC whose properties are reported above. The molecular weight of CEC2 (60 000, $f_{PE} = 0.25$ by weight) was chosen so that the PCHE and PE domain sizes would approximately match the small domain sizes of the CECEC. The triblock copolymer CEC2 deforms by crazing, and its median strain to fibril breakdown is approximately 1%, nearly as low as the PCHE homopolymer. However, as shown in Figure 10, once about 40% CECEC is added to the CEC2, the median strain to fibril breakdown begins to increase, and when 70% CECEC is added, no fibril breakdown or craze fracture is observed before the copper grid fails. These results show convincingly that it is the presence of the midblock chains in the CECEC that are responsible for the remarkable improvement in fracture properties of the pentablock copolymer over the triblock copolymer. This result points to the importance of developing block copolymer architectures that maximize chain bridging.[30]

Concluding Remarks

We have compared the morphology and microscopic aspects of the plastic deformation and fracture behavior of homopolymer PCHE, triblock copolymer CEC and pentablock copolymer CECEC using reflection optical microscopy, transmission electron microscopy, and scanning force microscopy. The homopolymer PCHE is susceptible to crazing and craze breakdown at low strains, leading to the brittle behavior expected for a glassy polymer with its high entanglement molecular weight of 49 000 g/mol. While the triblock copolymer shows modest increases in craze fibril stability even though its PCHE blocks are so short to be unentangled, a surprising improvement in resistance to crack formation is seen for the pentablock copolymer whose PCHE blocks are shorter still. This remarkable toughness is attributed to the presence of midblock chains that bridge between cylindrical PE domains, thus preventing the easy formation of voids and cracks in the PCHE matrix.

Acknowledgment. We acknowledge the primary financial support of the NSF under Award DMR-9632716 through the Materials Research Lab at UCSB. This work was also supported by a gift from Dow Chemical Co. We thank Prof. Frank S. Bates for many stimulating discussions on the morphology and macroscopic fracture behavior of these materials.

References and Notes

(1) Kramer, E. J.; Berger, L. L. *Adv. Polym. Sci.* **1990**, *91/92*, 1−68.

(2) Henkee, C. S.; Kramer, E. J. *J. Polym. Sci., Part B: Polym. Phys.* **1984**, *22*, 721−737.

(3) Donald, A. M.; Kramer, E. J. *J. Mater. Sci.* **1982**, *17*, 1871−1879.

(4) Bates, F. S.; Fredrickson, G. H. *Phys. Today* **1999**, *52*, 32−38.

(5) Hamley, I. W. *The Physics of Block Copolymers*; Oxford University Press: Oxford, 1998.

(6) Weidisch, R.; Michler, G. H.; Fischer, H.; Arnold, M.; Hofmann, S.; Stamm, M. *Polymer* **1999**, *40*, 1191−1199.

(7) Weidisch, R.; Schreyeck, G.; Ensslen, M.; Michler, G. H.; Stamm, M.; Schubert, D. W.; Budde, H.; Horing, S.; Arnold, M.; Jerome, R. *Macromolecules* **2000**, *22*, 5495−5504.

(8) Ryu, C. Y.; Lee, M. S.; Hajduk, D. A.; Lodge, T. P. *J. Polym. Sci., Part B: Polym. Phys.* **1997**, *35*, 2811−2823.

(9) Weimann, P. A.; Hajduk, D. A.; Chu, C.; Chaffin, K. A.; Brodil, J. C.; Bates, F. S. *J. Polym. Sci., Part B: Polym. Phys.* **1999**, *37*, 2053−2068.

(10) Quiram, D. J.; Register, R. A.; Marchand, G. R. *Macromolecules* **1997**, *30*, 4551−4558.

(11) Gehlsen, M. D.; Bates, F. S. *Macromolecules* **1993**, *26*, 4122−4127.

(12) Zhao, J.; Hahn, S. F.; Hucul, D. A.; Meunier, D. M. *Macromolecules* **2001**, *34*, 1737−1741.

(13) Bates, F. S.; Fredrickson, G. H.; Hucul, D.; Hahn, S. F. *AIChE J.* **2001**, *47*, 762−765.

(14) Fetters, L. J.; Lohse, D. J.; Richter, D.; Witten, T. A.; Zirkel, A. *Macromolecules* **1994**, *27*, 4639−4647. M_e of PCHE is 49 000 g/mol by recalculation of Fetters et al. data using $M_e = \rho RT/G_N$.

(15) Hucul, D. A.; Hahn, S. F. *Adv. Mater.* **2000**, *12*, 1855−1858.

(16) Brown, H. R. *J. Mater. Sci.* **1979**, *14*, 237−239.

(17) Lauterwasser, B. D.; Kramer, E. J. *Philos. Mag.* **1979**, *39A*, 469−395.

(18) Magonov, S. N.; Reneker, D. H. *Annu. Rev. Mater. Sci.* **1997**, *27*, 175−222.

(19) Magonov, S. N.; Elings, V.; Whangbo, M. H. *Surf. Sci.* **1997**, *375*, L385−L391.

(20) Mansky, P.; Russell, T. P.; Hawker, C. J.; Pitsikalis, M.; Mays, J. *Macromolecules* **1997**, *30*, 6810−6813.
(21) Huang, E.; Russell, T. P.; Harrison, C.; Chaikin, P. M.; Register, R. A.; Hawker, C. J.; Mays, J. *Macromolecules* **1998**, *31*, 7641−7650.
(22) Donald, A. M.; Kramer, E. J. *J. Polym. Sci., Part B: Polym. Phys.* **1982**, *20*, 899.
(23) Donald, A. M.; Kramer, E. J. *Polymer* **1982**, *23*, 461−465.
(24) Yang, A. C. M.; Kramer, E. J.; Kuo, C. C.; Phoenix, S. L. *Macromolecules* **1986**, *19*, 2010−2019.
(25) Ruokolainen, J.; Ryu, C. Y.; Magonov, S. N.; Hahn, S. F.; Fredrickson, G. H.; Kramer, E. J., manuscript in preparation.
(26) Ryu, C. Y.; Fredrickson, G. H.; Kramer, E. J.; Hahn, S. F.; Magonov, S. N., manuscript in preparation.
(27) Matsen, M. W.; Thompson, R. B. *J. Chem. Phys.* **1999**, *111*, 7139−7146.
(28) Creton, C.; Kramer, E. J.; Hui, C. Y.; Brown, H. R. *Macromolecules* **1992**, *25*, 3075−3088.
(29) Weimann, P. A. Ph.D. Thesis, University of Minnesota, Minneapolis, 1998.
(30) Drolet, F.; Fredrickson, G. H. *Macromolecules* **2001**, *34*, 5317−5324.

MA011576R